

Table S1.**Wettability and free surface energy of test substrates.**

The contact angle measuring device OCAH200 and SCA20 3.7.4 software (Data-Physics Instruments GmbH, Filderstadt, Germany) were used to estimate the wettability of test substrates by contact angle (CA) measurements. The free surface energy (FSE), its polar (p) and disperse (d) portions were calculated. For detailed description of the method see [Voigt and Gorb \(2010\)](#).

Substrate	FSE	Polar component	Disperse component	CA of Aqua millipore water
<u>Substrates used in inversion and traction tests</u>				
Glass	52.4 mN mm ⁻¹	36.5 mN mm ⁻¹	15.9 mN mm ⁻¹	39.3°
Silicone	7.2 mN mm ⁻¹	0.5 mN mm ⁻¹	6.8 mN mm ⁻¹	123°
Spurr resin	27.2 mN mm ⁻¹	4.0 mN mm ⁻¹	23.2 mN mm ⁻¹	91.3°
Native skin*	25-29 mN mm ⁻¹	10.8 mN mm ⁻¹	16.2 mN mm ⁻¹	80-110°
<u>Substrates used in centrifugal force test</u>				
Normal glass	52.0 mN mm ⁻¹	34.6 mN mm ⁻¹	17.4 mN mm ⁻¹	42°
Silanized glass	11.4 mN mm ⁻¹	1.8 mN mm ⁻¹	9.6 mN mm ⁻¹	108°

*according to [Ginn et al. \(1968\)](#); [Czech et al. \(2011\)](#); [Persson et al. \(2013\)](#)

References

- Czech, Z., Kowalczyk, A. and Swiderska, J.** (2011). Pressure-sensitive adhesives for medical applications. In *Wide Spectra of Quality Control* (ed. I. Akyar), pp. 1-25. Intechopen. doi:10.5772/23827.
- Ginn, M. E., Noyes, C. M. and Jungermann, E.** (1968). The contact angle of water on viable human skin. *J. Colloid Interface Sci.* **26**, 146-51. doi:10.1016/0021-9797(68)90306-8.
- Persson, B. N. J., Kovalev, A. and Gorb, S. N.** (2013). Contact mechanics and friction on dry and wet human skin. *Tribol. Lett.* **50**, 17-30. doi:10.1007/s11249-012-0053-2.
- Voigt, D. and Gorb, S.** (2010). Egg attachment of the asparagus beetle *Crioceris asparagi* to the crystalline waxy surface of *Asparagus officinalis*. *Proc. R. Soc. B* **277**: 895-903. doi:10.1098/rspb.2009.1706.

Table S2.Mean length and width [μm] of leg segments and total legs, $n=2$ per leg number.

Sex	Podomere	L IV		L III		L II		L I		Pooled mean	
		Length	Width	Length	Width	Length	Width	Length	Width	Length	Width
F	Coxa	333.86	277.84	363.29	245.13	349.54	196.31	350.28	201.26	349.24	230.14
E	Trochanter	347.43	157.44	266.57	169.32	228.82	162.00	209.47	176.78	263.07	166.38
M	Femur	590.99	135.46	418.27	155.08	373.6	145.08	494.45	161.09	469.33	149.18
A	Patella	548.62	156.07	454.52	170.93	381.84	145.48	486.84	162.41	467.96	158.73
L	Tibia	450.39	133.78	370.08	162.41	361.31	143.27	425.99	154.66	401.94	148.53
E	Tarsus	657.74	107.32	561.74	126.70	490.68	127.22	728.01	144.28	609.54	126.38
	Total leg length	2929.0		2434.5		2185.8		2695.0		2561.1	
	Mean leg width		161.3		171.6		153.2		166.8		163.2
M	Coxa	138.13	300.78	149.33	252.19	162.08	189.03	215.05	200.67	166.15	235.67
A	Trochanter	140.34	267.09	179.60	162.79	120.14	138.91	178.22	147.38	154.57	179.04
L	Femur	183.33	156.94	313.59	120.25	270.02	120.10	395.83	144.14	290.69	135.36
E	Patella	277.14	136.56	357.21	146.13	272.49	144.35	361.79	158.80	317.16	146.46
	Tibia	421.21	107.63	256.54	124.14	230.11	133.31	324.61	149.90	308.12	128.75
	Tarsus	399.07	140.30	442.61	112.02	385.79	129.72	625.90	135.65	463.34	129.42
	Total leg length	1559.2		1698.9		1440.6		2101.4		1700.0	
	Mean leg width		184.9		152.9		142.6		156.1		159.1

Table S3.

Area of the pad [μm^2] in contact with a glass slide, while tick is attached to the ceiling. Data on left and right legs are pooled together (mean \pm standard deviation). Asterisks: statistical differences between unfolded and folded pads for a single leg. Lower case letters: statistical differences between legs I-IV at the same condition (single row). Upper case letters: statistical differences between male and female for a single leg at the same condition.

Leg no.	I	II	III	IV
Male				
Unfolded	6902.0 \pm 1304.28 A	6581.5 \pm 285.59 *, A	6348.0 \pm 231.61 *, A	6837.8 \pm 527.09 *, A
Expanded	18972.6 \pm 294.66 a	10050.6 \pm 186.64 b, *	9485.9 \pm 1436.81 b, *, A	8885.4 \pm 1616.18 b, *
Female				
Unfolded	10054.4 \pm 58.75 a, B	9090.9 \pm 851.24 ab, *, B	7462.8 \pm 683.55 b, *, B	9338.5 \pm 842.06 a, *, B
Expanded	25237.6 \pm 10511.56 a	13006.1 \pm 1234.18 ab, *	11486.1 \pm 178.62 b, *, B	10847.8 \pm 514.72 b, *

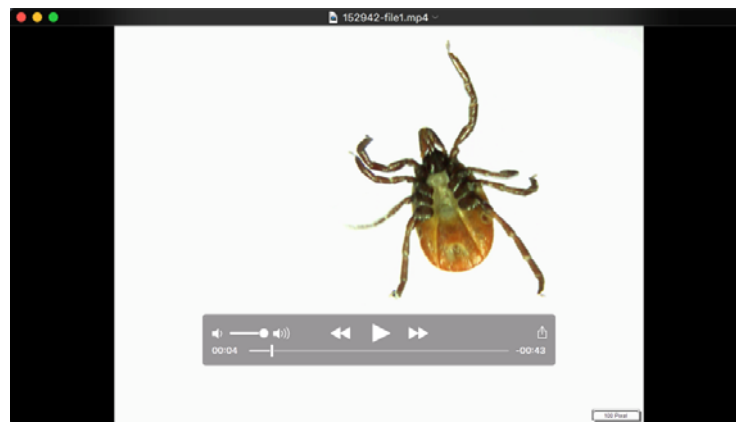
Further results of statistical processing.

Male: expanded pad, differences between legs (one-way ANOVA, $F_{3,9}=56.2$, $P<0.001$, followed by all pairwise multiple comparison procedure Dunn's test, $P<0.05$); unfolded vs. unexpanded, leg II (t -test, $t=-346$, $P\leq 0.001$), leg III (t -test, $t=-6.2$, $P\leq 0.001$), leg IV (t -test, $t=-2.8$, $P=0.047$).

Female: unfolded pad, differences between legs (one-way ANOVA, $F_{3,21}=5.6$, $P=0.006$, followed by all pairwise multiple comparison procedure Dunn's test, $P<0.05$); expanded pad, differences between legs (Kruskal-Wallis one-way ANOVA on ranks, $H_{3,34}=13.4$, $P=0.004$, followed by all pairwise multiple comparison procedure Dunn's test, $P<0.05$); unfolded vs. unexpanded condition, leg II (t -test, $t=-3.7$, $P=0.002$), leg III (t -test, $t=-7.7$, $P<0.001$), leg IV (Mann-Whitney rank sum test, $T=58$, $P=0.022$).

Male vs. female: leg I unfolded (Mann-Whitney rank sum test, $T=21$, $P=0.036$), leg II unfolded (Mann-Whitney rank sum test, $T=34$, $P=0.035$), leg III unfolded (t -test, $t=2.6$, $P=0.021$), leg IV unfolded (t -test, $t=3.4$, $P=0.020$), leg III expanded (t -test, $t=3.0$, $P=0.020$).

Area of the pads in contact, all legs pooled together,
 unfolded: 26669 μm^2 in males, 35947 μm^2 in females;
 expanded: 47395 μm^2 in males, 60578 μm^2 in females.



Movie 1.

Females of *Ixodes ricinus* walking on the glass ceiling. Pads while getting in contact and detachment are visible; 3.3 times decelerated.

1st sequence: A female walking on a glass surface at ceiling position.

2nd sequence: Attachment and detachment of translucent adhesive pads during locomotion are visible. The totally expanded adhesive pad of a second leg in contact with a glass surface while tick remained at ceiling position. The process of detachment of the pad is visualized.

3rd sequence: The folded adhesive pad of a foreleg in contact with a glass surface while tick remained at ceiling position. The process of detachment of the pad is visualized. After detachment, a residue of adhesion-mediating fluid is detectable.

4th sequence: The slightly unfolded adhesive pad of a hindleg in contact with a glass surface while tick remained at ceiling position. Tuning of attachment by alteration of the pad area is visible. By pulling the leg, the pad is more folded (claws fold together). By pushing the leg, the pad unfolds while its area increases (claws spread apart).